Neuron, Vol. 45, 861–872, March 24, 2005, Copyright ©2005 by Elsevier Inc. DOI 10.1016/j.neuron.2005.02.006

Regulation of Gene Expression by Lithium and Depletion of Inositol in Slices of Adult Rat Cortex

Philip E. Brandish,[1,*] Ming Su,[1] Daniel J. Holder,[1] Paul Hodor,[1] John Szumiloski,[1] Robert R. Kleinhanz,[2] Jaime E. Forbes,[2] Mollie E. McWhorter,[2] Sven J. Duenwald,[2] Mark L. Parrish,[2] Sang Na,[1] Yuan Liu,[1] Robert L. Phillips,[1] John J. Renger,[1] Sethu Sankaranarayanan,[1] Adam J. Simon,[1] and Edward M. Scolnick[3]

[1]Merck & Co., Inc.
West Point, Pennsylvania 19486
[2]Rosetta Inpharmatics LLC, a wholly owned subsidiary of Merck & Co. Inc.
401 Terry Avenue North
Seattle, Washington 98011

Summary

Lithium inhibits inositol monophosphatase at therapeutically effective concentrations, and it has been hypothesized that depletion of brain inositol levels is an important chemical alteration for lithium's therapeutic efficacy in bipolar disorder. We have employed adult rat cortical slices as a model to investigate the gene regulatory consequences of inositol depletion effected by lithium using cytidine diphosphoryl-diacylglycerol as a functionally relevant biochemical marker to define treatment conditions. Genes coding for the neuropeptide hormone pituitary adenylate cyclase activating polypeptide (PACAP) and the enzyme that processes PACAP's precursor to the mature form, peptidylglycine α-amidating monooxygenase, were upregulated by inositol depletion. Previous work has shown that PACAP can increase tyrosine hydroxylase (TH) activity and dopamine release, and we found that the gene for GTP cyclohydrolase, which effectively regulates TH through synthesis of tetrahydrobiopterin, was also upregulated by inositol depletion. We propose that modulation of brain PACAP signaling might represent a new opportunity in the treatment of bipolar disorder.

Introduction

Bipolar disorder (BD) is a chronic psychiatric illness characterized by recurrent episodes of depression and mania with prevalence estimated at 1%–2% lifetime risk in the United States (DSM-IV, 1994; Weissman et al., 1988). Lithium is effective at stabilizing mood, reducing the rate of relapse, and reducing suicide in BD (Burgess et al., 2003; Dinan, 2002; Goodwin et al., 2003). Although valproate and lamotrigine have been introduced as maintenance therapies with efficacy demonstrated in clinical trials, lithium is still a front-line treatment for BD, despite significant side effects (Bowden et al., 2000; Bowden et al., 2003; Dinan, 2002). The etiology of the disease and the mechanism of action of lithium remain to be determined, and this has understandably stifled development of safer, more effective medicines.

There are numerous hypotheses for the mechanism of action of lithium in BD, and these have been reviewed (Gould et al., 2004; Gurvich and Klein, 2002). Glycogen synthase kinase 3 (GSK3) and inositol monophosphatase (IMPase) are both inhibited by lithium and have been topics of considerable study as potential therapeutic targets in BD.

An effect of lithium on brain inositol levels was demonstrated more then 30 years ago (Allison and Stewart, 1971). Inositol phosphates and inositol-containing phospholipids (phosphoinositides) constitute an array of cell signaling molecules with diverse functions (Irvine and Schell, 2001; Majerus, 1992). Most notably, activation of cell surface receptors can activate hydrolysis of phosphatidylinositol-4,5-bisphosphate (PIP_2) by phospholipase C (PLC) to produce inositol-1,4,5-trisphosphate (IP_3), which is a second-messenger molecule. IP_3 binds to its cognate receptor to trigger release of Ca^{2+} from the endoplasmic reticulum (ER) and a host of downstream signaling events. Lithium inhibits two enzymes in the inositol pathway, namely inositol polyphosphate 1-phosphatase and IMPase, both uncompetitively with respect to substrate (Majerus, 1992). Indeed, therapeutically relevant doses of lithium cause accumulation of inositol phosphates in the brains of rats and mice (Atack et al., 1992; Sherman et al., 1986). The "inositol depletion" hypothesis of lithium's action in BD was formulated by Berridge (Berridge et al., 1989). Simply put, lithium blocks IMPase and the recycling of inositol into inositol lipids. This leads to a reduction in PIP_2 and a reduction in the ability of the cell (neuron) to respond to a stimulus by making IP_3 to stimulate an increase in intracellular Ca^{2+} concentration. Thus, neuronal excitability is reduced, and this somehow leads to normalization of mood. Further, the hypothesis says that because brain cells have limited access to dietary inositol they are more dependent on recycled inositol than cells in the periphery, giving rise to a therapeutic window (Berridge et al., 1989, and references therein).

There is a delay of 5–10 days between commencement of lithium therapy and therapeutic benefit (Lenox and Manji, 1998). The basis for this is unknown, but it is credible that gene regulatory events and subsequent changes in protein expression are required. The beneficial effect of lithium in BD may be derived from a combination of GSK3- and inositol-mediated events, meaning that both pathways need to be studied and their contributions dissected by performing experiments with lithium under inositol-depleted and inositol-replete conditions. In yeast cells, a pathway regulated by inositol levels is emerging. However, in mammalian cells much less is known (Loewen et al., 2004; Schuller et al., 1995). In the present work, we have focused our effort on identifying genes whose expression levels are changed by lithium's action on the inositol pathway.

*Correspondence: philip_brandish@merck.com
[3]Present address: The Broad Institute, One Kendall Square, Cambridge, Massachusetts 02139.

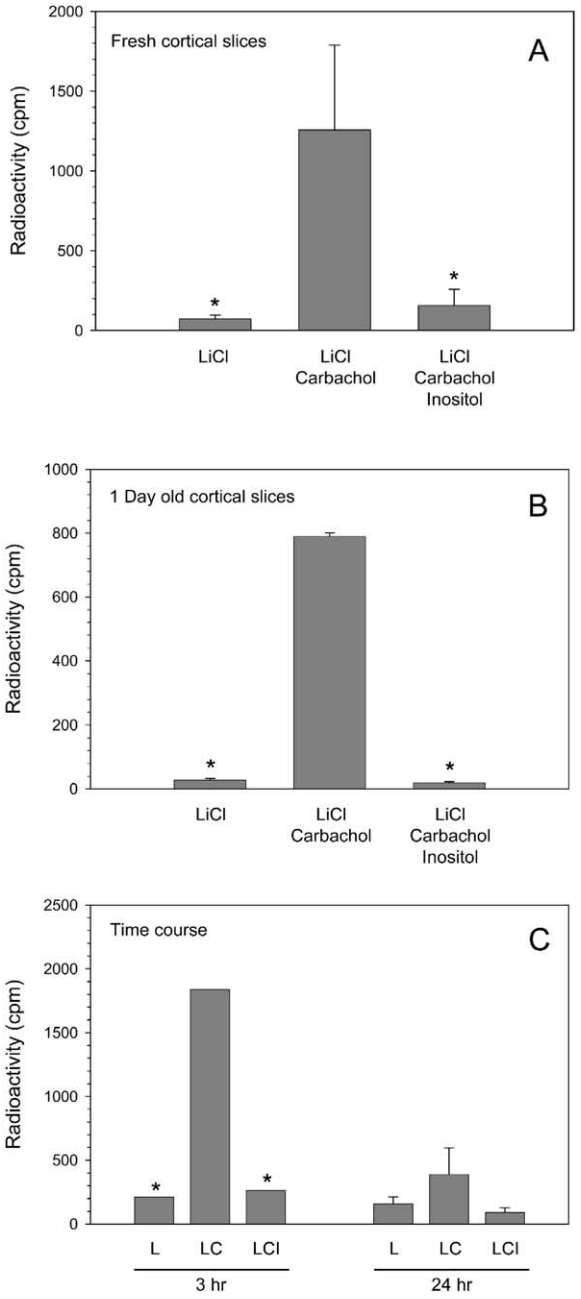

Figure 1. Accumulation of CDP-DAG in Adult Rat Brain Cortical Slices

Slices were prepared and dispensed two per well into culture medium containing 2 mM LiCl as described in the Experimental Procedures section. Tritiated cytidine, carbachol, and inositol were added as described for each panel, t = 0 being the time at which the slices were dispensed to the medium. At the indicated time, the tissue was removed and CDP-DAG estimated as the amount of organic solvent-extractable radioactivity. Statistical analysis was performed using ANOVA followed by Tukey's post test: *p < 0.01 versus LiCl + carbachol treatment. (A) Where indicated in the figure, 10 mM inositol was added at t = 0, 10 μCi of ^{3}H-cytidine at t = 1 hr, carbachol to 50 μM at t = 2 hr. At t = 3 hr, tissue was processed for analysis of CDP-DAG. Data shown are means (n = 4) ± SD. (B) Where indicated in the figure, 10 mM inositol was added at t = 0, 10 Ci of ^{3}H-cytidine at t = 22 hr, carbachol to 50 μM at t = 23 hr. At t = 24 hr, tissue was processed for analysis of CDP-DAG. Data shown are means (n = 3) ± SD. (C) Where indicated in the figure, 10 mM inositol was added at t = 0, 10 μCi of ^{3}H-cytidine at t = 1 hr, carbachol to 50 μM at t = 2 hr. At t = 3 or 24 hr, tissue was processed for analysis of CDP-DAG. Data shown are means (n = 2 for 3 hr, n = 3 for 24 hr) ± SD. For the 24 hr data, the effect of treatment was not significant: ANOVA p = 0.064. The individual values for the LiCl + carbachol group at 24 hr were 153, 556, and 454 cpm.

Inositol is present at high (millimolar) concentrations in the brain (Lubrich et al., 1997), such that a modest reduction in its concentration does not necessarily mean it has become a limiting metabolite. When inositol becomes limiting in the synthesis of phosphatidylinositol (PI) by PI synthase, cytidine diphosphoryl-diacylglycerol (CDP-DAG) accumulates, and particularly so when a cell (or brain slice) has been activated to produce IP_3 and DAG from PIP_2 (PI turnover) in the presence of lithium (Godfrey, 1989; Stubbs and Agranoff, 1993). CDP-DAG accumulation is therefore a surrogate marker for functional inositol depletion, and it is readily measurable by radiolabeling with ^{3}H-cytidine. Stimulation of PI turnover via agonism of muscarinic receptors with carbachol is one approach that has been used widely to study the PI pathway and can similarly be used to study modulation of neuronal (and brain) signaling caused by inhibition of IMPase, in this case by lithium. Stubbs and Agranoff have demonstrated accumulation of CDP-DAG in acute (1–2 hr) studies using cross-chopped slices of adult rat cortex treated with carbachol and LiCl (Stubbs and Agranoff, 1993). Adult rat cortical slices thus constitute a potential model for profiling the gene regulatory consequences of inositol depletion where the treatments used can be directed by a relevant biochemical marker, i.e., CDP-DAG.

Results

Acute Rat Brain Cortical Slices as an Ex Vivo Model of Brain Inositol Depletion

There is little precedent for extended, multiday culture of adult rat cortical slices. Therefore, we selected 24 hr as a time frame which would be long enough for gene expression changes to occur, but short enough that the slices could survive while still being relevant to the clinical disorder. This time frame is relevant because although symptomatic relief takes 5–10 days to occur, we expected, based on literature precedent, that inositol depletion would occur rapidly in the presence of carbachol and LiCl (e.g., <1 hr), leaving almost the entire time course for gene expression change. In contrast, symptomatic relief requires several events, including drug accumulation, biochemical change, gene regulatory change, and manifestation of benefit, each of which may take 1–2 days or more. To characterize the experimental system, we measured CDP-DAG accumulation with different treatments and at different times, isolated and quality tested total RNA, and imaged slices stained with propidium iodide or Hoechst 33342.

The goal of the experiment was to identify genes that are regulated as a consequence of inositol depletion due to blockade of inositol phosphatases by lithium in

the presence of an agonist that activates the PI pathway. Such genes would be up- or downregulated by treatment with LiCl and carbachol versus LiCl alone, and that regulation would be wholly or partially prevented by addition of excess inositol. Therefore, we measured accumulation of CDP-DAG in fresh and DIV1 slices treated with such combinations of LiCl, carbachol, and inositol (Figure 1). Concentrations of lithium associated with efficacy in bipolar disorder are in the 0.5–1.5 mM range (Lenox and Manji, 1998). In the presence of 2 mM LiCl, treatment of fresh slices with 50 μM carbachol caused a robust accumulation of CDP-DAG, which was completely prevented by inclusion of 10 mM inositol in the culture medium (Figure 1A). The same pattern of CDP-DAG accumulation was observed when the same treatments were applied at DIV1, although the amount of radioactivity measured in the slices treated with LiCl and carbachol was less than in fresh slices (Figure 1B). These data indicate that the biochemical function of the slices is preserved at DIV1. We also investigated the time course of CDP-DAG accumulation (Figure 1C). Fresh slices were labeled with ^{3}H-cytidine and treated with combinations of LiCl, carbachol, and inositol, and the amount of CDP-DAG was measured (as radioactivity) at 1 or 22 hr after addition of carbachol. The amount of CDP-DAG in slices treated with LiCl + carbachol appeared to be elevated after 22 hr compared to LiCl alone, or LiCl + carbachol + inositol, although a treatment effect did not reach statistical significance. A reduced amount of radiolabeled CDP-DAG could result from increased de novo inositol synthesis, but alternatively could be due to metabolism or other degradation of the radiolabeled species to effectively wash out the radiolabel.

Preliminary studies found that total RNA isolated from slices maintained in the presence of 1 mM LiCl was of consistent and acceptable quality (28S/18S ratio > 0.8, Rosetta Bioinformatics standard quality control metric), whereas total RNA isolated from slices maintained in the absence of LiCl was always severely degraded and low in yield (data not shown). We took this to be a manifestation of the well-documented protective properties of LiCl against neurotoxic insults such as those that occur during slice preparation, e.g., hypoxia and glutamate release (Jope and Bijur, 2002; Nonaka et al., 1998; Ren et al., 2003), and as a positive indication of slice viability. This led us to the treatment set design used in the experiments noted so far (LiCl, LiCl + carbachol, LiCl + carbachol + inositol) instead of the intuitive configuration (carbachol, carbachol + LiCl, carbachol + LiCl + inositol). Analysis of RNA samples from slices from one of the two animals that were used in the microarray study described below are shown in Figure 2. ANOVA found no significant effect ($p > 0.05$) of treatments on yield or 28S/18S ratio for this sample set. The same was true for a combined analysis of all six RNA sample sets used in this work.

We attempted to assess the viability of freshly prepared and 1-day-old drug-treated brain slices by staining them with propidium iodide, a membrane-impermeable dye that only stains nonviable cells, or with Hoechst 33342, which stained DNA from all cells (Bonde et al., 2002; Kristensen et al., 2003). Z series of images were acquired using confocal microscopy from

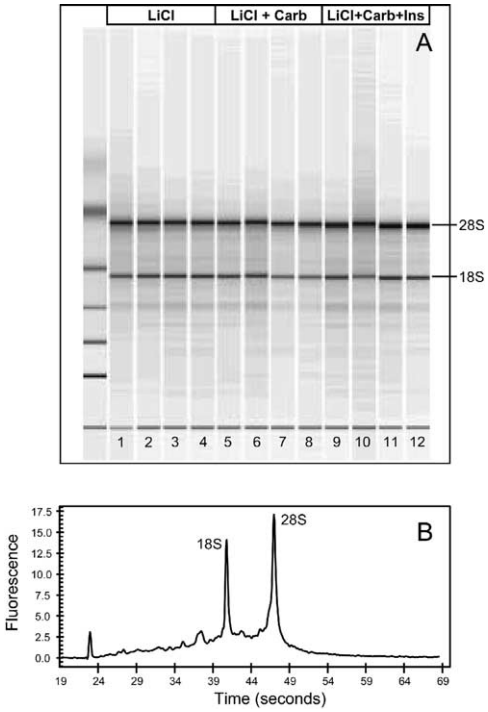

Figure 2. Adult Rat Brain Cortical Slice RNA Quality Control Data

(A) Pseudo-gel image of RNA samples extracted from slices treated for 24 hr with 2 mM LiCl (lanes 1 through 4), 2 mM LiCl + 50 μM carbachol (lanes 5 - 8), or 2 mM LiCl + 50 μM carbachol + 10 mM inositol (lanes 9 through 12). Purified total RNA was electrophoresed on an Agilent BioAnalyzer using a Nano RNA chip.

(B) Electropherogram of a single RNA sample from a pair of slices treated with 2 mM LiCl + 50 μM carbachol.

outer cortical regions under all conditions (due to ease of identification of this region) to compare the number of nuclei labeled for each treatment. Representative maximum projection images illustrate nuclear staining of freshly isolated brain slices stained with Hoechst or propidium iodide (Figure 3A). We observed Hoechst staining up to 60–80 μm within slices, while propidium iodide penetrated slices only to a depth of 30–40 μm, and so z series of images were obtained only to a depth of 40 μm for both staining conditions (Figure 3B). It should be noted that the surface of the slice was expected to contain a substantial proportion of nonviable cells due to the mechanical trauma of slice preparation and that this method is limited in that it does not give information about the viability of cells deeper within the slice (total 350 μm). The considerable variability in the number of Hoechst-labeled cells (i.e., total cell number) per image area from slice to slice precluded reliable estimation of the viable to nonviable ratio (Figure 3C). Although ANOVA detected a significant difference in the number of propidium iodide-stained cells between day 1 LiCl + carbachol + inositol and fresh or day 1 LiCl slices, the data do not point to a progressive deterioration during the 24 hr incubation or deterioration specifically associated with prolonged treatment with carbachol.

These three avenues of data led us to conclude that

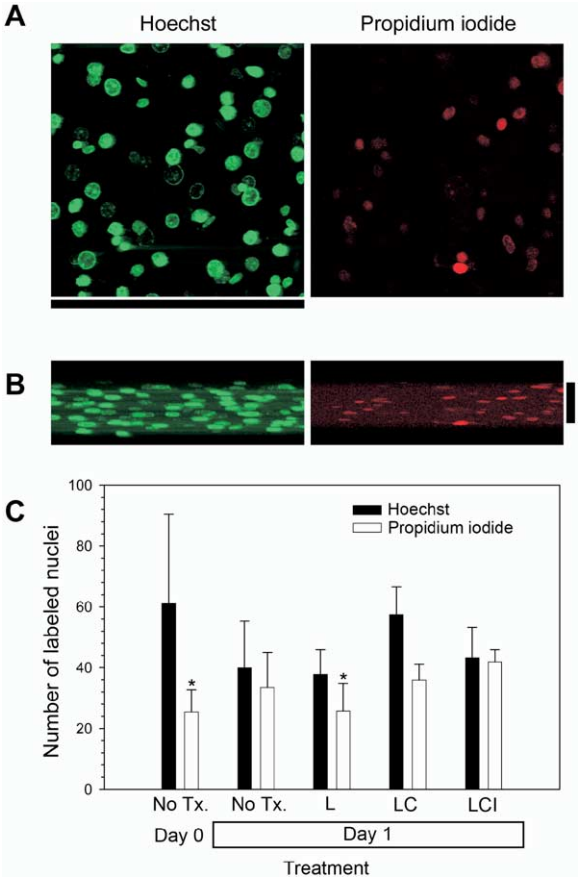

Figure 3. Confocal Imaging of Rat Brain Cortical Slices

(A) Maximum-intensity projection from a representative slice stained immediately following sectioning at day 0. The nuclei in the Hoechst-stained section is pseudocolored green, while the propidium iodide-stained section is pseudocolored red. Scale bar, 155 μm.

(B) A maximum projection tilt series was created from the same slice as in (A) to visualize slice thickness from a side-on view perpendicular to the plane of the slice. Scale bar, 30 μm.

(C) The number of labeled nuclei measured in Hoechst- (dark bar) and PI-stained (clear bar) sections from day 0 and day 1 slices following different treatments. No Tx., no treatment; L, 2 mM LiCl; LC, 2 mM LiCl + 50 μM carbachol; LCI, 2 mM LiCl + 50 μM carbachol + 10 mM inositol. The data are means ± SD from four to six regions from n = 3 slices for each condition. The number of nuclei labeled with Hoechst was not statistically different among the different treatment groups ($p > 0.05$ ANOVA and Student's t test). The LiCl only and the day 0 cultures showed significantly less labeling compared to the LCI condition ($p < 0.05$ by ANOVA followed by Tukey's post test).

in rat brain cortical slices maintained in the manner described, and perturbed with the treatments described, integrity and function at DIV1 was sufficient to warrant proceeding with the microarray analysis of the RNA samples collected.

Microarray Identification of Candidate Inositol-Regulated Genes

The three different treatments, 2 mM LiCl (L), 2 mM LiCl + 50 μM carbachol (LC), and 2 mM LiCl + 50 μM carbachol + 10 mM inositol (LCI), were carried out with

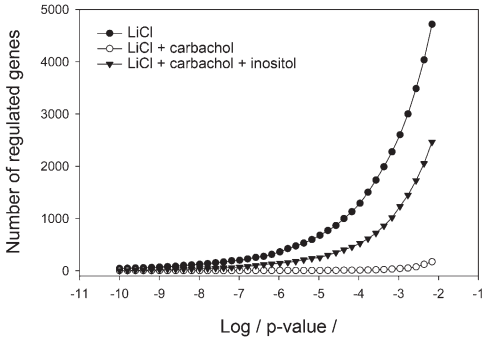

Figure 4. Global Preliminary Assessment of the Microarray Data Set

The number of statistically significantly regulated genes in each treatment group versus the LiCl + carbachol pool sample at varying cut off levels for significance. For any given cut off p value, the number of genes significantly regulated in the LiCl + carbachol treatment group represents the false-positive rate. The numbers of significantly regulated genes in the LiCl and LiCl + carbachol + inositol groups are several-fold larger than the false-positive rate, irrespective of the p value used to determine significance.

four replicates each. The experiment was performed with two animals, on separate days, ultimately yielding a total of 24 RNA samples (two animals × three treatments × four biological replicates). We used a two fluor, two color, cohybridization microarray technology, where the output is the log of the ratio of the expression level of a given gene in one sample relative to the same gene in a second sample. Since the LC treatment condition is different from the other two by one variable, we designated that as the control treatment for the purpose of the microarray experiment even though conceptually L and LCI are control (inositol replete) states and LC is the perturbed state (inositol depleted). This experimental design then makes two comparisons: L versus LC, and LCI versus LC. In fact, we took a small portion of each of the eight LC samples and pooled them to make a reference sample. Each individual RNA sample would then be compared to the pool-of-LC reference sample. This includes the individual LC samples, which allowed us to include the sample-to-sample variability of the LC group in our statistical testing.

RNA was amplified using a two-round reverse transcription/in vitro transcription protocol and dye labeled. Each amplified, labeled RNA sample was compared to the LC reference sample by cohybridization to custom-made Agilent oligonucleotide arrays (designated Rat 50k v2.1 Array 1) with one fluor-reversed pair (FRP) for each sample. Differential expression in the test sample versus LC reference sample was expressed as the logarithm of the ratio of signal in the sample channel to signal in the control pool channel (log ratio). A reporter is defined as the 60-mer oligonucleotide that is present on the microarray chip. A single gene may be represented in the array by more than one reporter. As a preliminary assessment of the microarray data we plotted the number of reporters for which the mean log ratio value was significantly different than zero (i.e., differentially regulated compared to the pool-of-LC reference sample) with an associated p value less than a set number over a range of arbitrarily set p values (Figure 4). This analysis immediately told us that the num-

bers of statistically significant differences between L and the pool-of-LC reference sample, and between LCI and the pool-of-LC reference sample were many fold greater than the differences between LC and the pool-of-LC reference sample (false positives) irrespective of the stringency of analysis. We also performed clustering analysis of the individual samples by log ratio value across reporters (Figure S1 in the Supplemental Data available with this article online). This analysis told us that the variability between animals/day-of-experiment was greater than the variability between treatment replicates from a single animal.

Given the properties of the microarray data, we elected to analyze the data segregated by animal as well as analyzing the combined data set. Note that the above analyses consider comparisons of treatment replicates versus LC reference pool and therefore do not take into account the variability in the LC treatment group. To identify regulated genes for further analysis, we must take the variability in the LC treatment group into account by comparing the log ratio values from the L group versus the log ratio values from the LC group, and similarly for the LCI group versus the LC group. A purely biological feature of this experiment is that inositol-responsive genes will only be regulated in those cells in the slice preparation where inositol is depleted, although secondary effects reaching other cells are possible. We therefore expect that any regulation will be diluted against the total compliment of mRNA for that gene present in the slice. Based on these considerations and on the preliminary characterization of the data, we set the following criteria for a reporter/gene to be considered "of interest":

1. $p < 0.05$ for both L versus LC and LCI versus LC in the data from the two animals combined.
2. $p < 0.224$ (square root of 0.05) for both L versus LC and LCI versus LC in the data from each animal.
3. Fold change $\geq$ 1.3 up or down (but in the same direction) for L versus LC and LCI versus LC in the data from the two animals combined.

We set rather low stringencies for individual comparisons and did not correct for multiple testing expecting that the false-positive rate would instead be minimized to a degree by the requirement for coincident regulation above the threshold magnitude (fold change $\geq$ 1.3) in both the L versus LC and LCI versus LC comparisons. Also, because we intended to do a confirmation study using real-time quantitative PCR, we were less concerned about minimizing false positives, but we were keen to minimize false negatives. The second criterion was included to avoid reporters/genes being indicated as significant in the aggregate solely on the basis of data from a single animal.

The criteria were satisfied for 173 reporters (171 genes). Probe sequences, gene symbols, and microarray results for all these genes are listed in Table S1, and a heatmap showing clustering by sample and by gene illustrates those data (Figure S2). These were considered candidate inositol-regulated genes. Among the 171 genes, 60 are known or could be annotated with confidence using public database information. The myristoylated alanine-rich C-kinase substrate (MARCKS) protein has been reported to be regulated by lithium in an inositol-dependent manner in immortalized hippocampal (HN33) cells (Wang et al., 2001). The MARCKS gene, the rat homolog being MARCKS-like protein (*Mlp*), was not found to be regulated by inositol depletion in this study. The microarray used included two separate reporters for *Mlp*.

Validation of Candidate Inositol-Regulated Genes Using Real-Time Quantitative PCR

The functionally annotated genes were selected for confirmation using real-time quantitative PCR (RT-QPCR), as well as two of the nonannotated sequences where the microarray data was highly statistically significant (*LOC286960* and *LOC140610*). For RT-QPCR analysis, we prepared new, independent RNA samples: four animals × three treatments × three biological replicates per animal. The yield of RNA from individual samples (average 2.1 μg total RNA) was insufficient for RT-QPCR analysis of 64 genes (60 test genes and 4 internal reference genes), so we amplified messenger RNAs using the aRNA method originally devised by Eberwine (Phillips and Eberwine, 1996). Three samples were not carried forward to RT-QPCR analysis because of no product or very low yield from the aRNA amplification procedure. Two of the annotated genes (*Cxadr* and *Sat*) were not included in the study because the RT-QPCR assay did not work in a pilot trial.

The RT-QPCR results are given in Table S3. Correlation between the RT-QPCR results and the microarray results was rather modest (Figure S3), but we attribute this to a high false-positive rate anticipated from our statistical cut-off values used in analysis of the microarray data and to the small fold changes measured (average of 1.6-fold in either direction for candidate inositol-regulated genes) rather than poor data quality. At this stage of the study, we were concerned to minimize the false-positive rate, that is, to be highly confident that the genes identified are specifically regulated by inositol depletion caused by LiCl and carbachol treatment. To this end, we set the following two criteria:

1. $p < 0.025$ for both LC versus L (inositol depletion) and LCI versus LC (inositol repletion).
2. Fold change $\geq$ 1.3 up or down (but in the opposite direction) for both LC versus L and LCI versus LC.

Twenty genes out of the 60 tested satisfied these criteria and are shown above the line in Table 1. Genes below the line do not meet the criteria set out above, but still had p values < 0.05 for both comparisons and so were not dismissed. As noted above in consideration of the correlation between the RT-QPCR data and the microarray data, this confirmation rate reflects the low stringency deliberately set for identification of candidate inositol-regulated genes in the microarray portion of the study. All of the confirmed genes were upregulated by inositol depletion and downregulated by inositol repletion, but not down- and upregulated, respectively. We are not aware of any bias or systematic error in the experiment, the technology, or the data analysis that would favor detection of genes upregu-

Table 1. RT-QPCR Results for Confirmed and "Near-Miss" Inositol-Regulated Genes

	Change in Inositol Status			
	Depletion (LC[a] versus L)		Repletion (LCI versus LC)	
Gene[b]	Fold Change	p Value	Fold Change	p Value
C4bpa	↑ 7.10	<0.0001	↓ 4.42	<0.0001
Sarcosin	↑ 7.71	<0.0001	↓ 2.77	<0.0001
Mustang	↑ 3.00	<0.0001	↓ 1.71	0.0009
Adcyap1	↑ 3.11	<0.0001	↓ 2.01	0.0010
Mmp12	↑ 5.53	<0.0001	↓ 2.33	0.0010
Nox1	↑ 2.98	<0.0001	↓ 2.14	0.0012
Edn2	↑ 6.81	<0.0001	↓ 3.53	0.0013
Mmp10	↑ 2.40	<0.0001	↓ 1.62	0.0015
Slc26a3	↑ 2.50	<0.0001	↓ 1.94	0.0016
Atf3	↑ 1.57	0.0004	↓ 1.47	0.0019
Gch	↑ 1.42	0.0038	↓ 1.52	0.0008
LOC286960	↑ 2.99	0.0038	↓ 3.80	0.0005
Gpr88	↑ 2.18	0.0060	↓ 2.30	0.0037
Cbr1	↑ 1.81	0.0067	↓ 1.78	0.0085
Crem-1	↑ 1.47	0.0006	↓ 1.31	0.0115
Cited2	↑ 1.67	0.0013	↓ 1.47	0.0120
MS1	↑ 4.24	<0.0001	↓ 1.98	0.0147
Filip	↑ 1.52	0.0172	↓ 1.50	0.0208
Kras2	↑ 1.49	0.0225	↓ 1.62	0.0064
Slc2a2	↑ 1.82	0.0245	↓ 1.86	0.0200
Pam	↑ 2.38	0.0005	↓ 1.66	0.0268
Tnfip6	↑ 2.21	<0.0001	↓ 1.36	0.0283
Kcna4	↑ 1.73	0.0175	↓ 1.65	0.0290
Hcn1	↑ 1.92	0.0308	↓ 2.08	0.0163
Arpp19	↑ *1.24*	*0.0309*	↓ *1.26*	*0.0221*
Rptpk	↑ 1.53	0.0046	↓ 1.35	0.0369
Rgs4	↑ 1.66	0.0390	↓ 1.69	0.0349
Stxbp5	↑ *1.29*	*0.0437*	↓ *1.37*	*0.0139*
Syt12	↑ *1.27*	*0.0490*	↓ *1.29*	*0.0357*

Genes names and data are italicized if the fold change for either comparison is <1.3.
[a] L, LiCl; LC, LiCl + carbachol; LCI, LiCl + carbachol + inositol.
[b] The data are ranked in ascending order by the numerically higher of the two p values associated with each gene.

lated by inositol depletion over downregulated genes. It is quite possible that this is a real biological phenomenon, and presently we have no reason not to believe this interpretation.

Table 2 lists the confirmed inositol-regulated genes, the human homologs, and the full name of the human homolog derived from the NIH/NCBI Entrez Gene web facility (http://www.ncbi.nlm.nih.gov/entrez/query.fcgi?db=gene) as well as synonyms. In addition to literature search evaluation of these newly identified inositol-regulated genes, we compared the cytogenetic location of the human homologs of the 20 confirmed inositol-regulated genes (as well as the "near-miss" genes) to a catalog of BD risk loci prepared from the literature. For inositol-regulated genes at or close to BD risk loci, we calculated the distance of the gene from the nearest risk locus, typically a sequence tagged site (STS) marker, based on chromosomal locations retrieved through the UC Santa Cruz Human Genome Browser Gateway (July 2003 assembly) at http://genome.ucsc.edu/. Two genes that had p values < 0.05 for both comparisons in the RT-QPCR study were located within 1 million base pairs (MB) of a bipolar disorder risk locus. *ADCYAP1* is one of six genes identified as possible risk genes in a recent study of bipolar I disorder in a Costa Rican population (McInnes et al., 2001). The ADCYAP1 gene is 0.26 MB from D18S59 (STS marker AFM178XC3) at chromosome 18p11.3, which was in linkage disequilibrium. Human *SLC26A3* is located at chromosome 7q31, and is 0.97 MB from D7S501 (STS marker AFM199VB2), which was identified as a risk locus marker by Detera-Wadleigh et al. in a genome scan of 22 bipolar disorder pedigrees (Detera-Wadleigh et al., 1999).

Specific transcription factors and a consensus inositol-choline promoter response element have been described in yeast that allow the organism to regulate genes according to cellular inositol levels (Schuller et al., 1995). Both lithium and valproate can regulate genes such as *INO1* and *INO2* in yeast via depletion of inositol (Vaden et al., 2001), and phosphatidic acid has very recently been identified as the effector molecule that couples inositol levels to regulation of transcription factor activity (Loewen et al., 2004). To the best of our knowledge, none of the yeast homologs of the genes listed in Table 1 have been shown to be regulated by inositol.

Discussion

Lithium acts on many molecular pathways in the brain, but in this gene expression profiling study we were able to specifically associate the regulation of genes with inositol depletion arising from blockade by LiCl of

Table 2. Annotation and Functional Summary of Confirmed Inositol-Regulated Genes

Rat Gene Symbol	Human Homolog	Full Name	Synonyms
C4bpa	C4BPA	complement component 4 binding protein, alpha	
Sarcosin	KBTBD10	kelch repeat and BTB (POZ) domain containing 10	Sarcosin
Mustang	MUSTN1	musculoskeletal, embryonic nuclear protein 1	mustang
Adcyap1	ADCYAP1	adenylate cyclase activating polypeptide 1 (pituitary)	PACAP
Mmp12	MMP12	matrix metalloproteinase 12 (macrophage elastase)	HME, MME
Nox1	NOX1	NADPH oxidase 1	GP91-2, MOX1, NOH-1, NOH1
Edn2	EDN2	endothelin 2	ET2
Mmp10	MMP10	Matrix metalloproteinase 10	Stromelysin 2, transin
Slc26a3	SLC26A3	solute carrier family 26, member 3 (sulfate)	CLD, DRA
Atf3	ATF3	activating transcription factor 3	
Gch	GCH1	GTP cyclohydrolase 1 (dopa-responsive dystonia)	DYT5, GCH, GTPCH1
LOC286960	not known	Preprotrypsinogen IV (rat only)	
Gpr88	GPR88	G-protein coupled receptor 88	STRG
Cbr1	CBR1	carbonyl reductase 1	
Crem (1)	CREM	cAMP responsive element modulator	ICER
Cited2	CITED2	Cbp/p300-interacting transactivator, with Glu/Asp-rich carboxy-terminal domain, 2	MRG1, P35SRJ
MS1	STARS	striated muscle activator of Rho-dependent signaling	
Filip	FILIP1	filamin A interacting protein 1	
Kras2	KRAS2	v-Ki-ras2 Kirsten rat sarcoma 2 viral oncogene homolog	C-K-RAS, K-RAS2A, K-RAS2B, K-RAS4A, K-RAS4B, KI-RAS, KRAS, RASK2
Slc2a2	SLC2A2	solute carrier family 2 (facilitated glucose transporter), member 2	GLUT2
Pam	PAM	peptidylglycine alpha-amidating monooxygenase	PAL, PHM
Tnfip6	TNFAIP6	tumor necrosis factor, alpha-induced protein 6	TSG6
Kcna4	KCNA4	potassium voltage-gated channel, shaker-related subfamily, member 4	HBK4, HK1, HPCN2, HUKII, KCNA4L, KCNA8, KV1.4, PCN2
Hcn1	HCN1	hyperpolarization activated cyclic nucleotide-gated potassium channel 1	BCNG-1, BCNG1, HAC-2
Arpp-19	ARPP-19	cyclic AMP phosphoprotein, 19 kD	ARPP-16, ARPP16, ARPP19
Rptpk	PTPRK	protein tyrosine phosphatase, receptor type, K	R-PTP-kappa
Rgs4	RGS4	regulator of G-protein signalling 4	RGP4
Stxbp5	STXBP5	syntaxin binding protein 5 (tomosyn)	LGL3, LLGL3
Syt12	SYT12	synaptotagmin XII	SRG1, SYT11

IMPase. Moreover, we can correlate the gene expression data with biochemical data that clearly demonstrate that the treatment conditions manipulate the slice preparation in the intended fashion. In this way, we know the proximal targeted biochemical pathway that leads to regulation of the genes, even though we do not yet know what signaling events lie in between.

Compared to many microarray studies, the number of genes confidently identified as regulated in this study may be deemed small. Several factors may contribute to this, including the high stringency that we set for confirmation and heterogeneity of the slice preparation leading to dilution of signal from cell type-specific events. Perhaps more significant though, the conditions of the study are rather specific in that to be called "regulated," a gene must be regulated by the action of carbachol in the presence of LiCl, and that regulation must be wholly or partially prevented by the addition of inositol. Because of these stringent conditions, and because the RT-QPCR study was performed using independent samples prepared several months after those used for microarray profiling, we have a very high degree of confidence in the results of this study. In the interest of brevity, we have focused discussion on inositol-regulated genes that by virtue of their function, and of independent findings, suggest new directions toward treatment of bipolar disorder. For example, GPR88 is an orphan GPCR that is expressed predominantly in the striatum and that bears highest homology to the serotonin 1D receptor among other GPCRs (Mizushima et al., 2000). A recent study showed expression of GPR88 to be regulated in rat prefrontal cortex in an animal model of mania and by valproate treatment, thus prioritizing this receptor for future study (Ogden et al., 2004).

Among the genes identified, we considered *ADCYAP1* especially interesting because it is a brain neuropeptide signaling molecule and because it is located close to a bipolar disorder risk locus on chromosome 18 (McInnes et al., 2001). *ADCYAP1* is the gene for pituitary adenylate cyclase activating polypeptide (PACAP), which is a brain neuropeptide that shares homology with vasoactive intestinal polypeptide (VIP) and acts through three different GPCRs (Vaudry et al., 2000). Although originally associated with the hypothalamus, subsequent studies showed widely distributed CNS expression, including the cerebral cortex, indicating a broader role than its name suggests (Mikkelsen et al., 1994; Skoglosa et al., 1999). PACAP knockout mice have a high neonatal mortality rate, but the surviving adult mice have a profound psychomotor phenotype, including general hyperactivity and explosive jumping behavior in a novel environment, and increased exploratory behavior associated with reduced anxiety (Hashimoto et al., 2001). These mice also exhibit circadian defects characterized by an attenuated phase advance

response to late subjective night light stimulation (Kawaguchi et al., 2003). Aberrant circadian behavior has been discussed as a pathological defect in bipolar disorder, and chronic lithium has been shown to regulate circadian behavior in animals (Lenox et al., 2002; Welsh and Moore-Ede, 1990). An independent knockout line was found to be cold sensitive, and results suggested that this was due to defects in catecholamine synthesis and thermoregulation (Gray et al., 2002). The *Drosophila* homolog of *PACAP* is *amnesiac*, for which loss-of-function mutation impairs learning and memory and causes increased ethanol sensitivity (Hashimoto et al., 2002). PACAP-specific receptor (Adcyap1r1, also called PAC_1) knockout mice show defects in associative fear learning, and PACAP has concentration-dependent effects on hippocampal synaptic plasticity (Hashimoto et al., 2002), but it remains to be seen if the PACAP knockout mice have learning and memory deficits also. Interestingly, peptidylglycine α-amidating monooxygenase (*Pam*) only very narrowly failed to meet our criteria to be confirmed as an inositol-regulated gene in the RT-QPCR study (Table 1). PAM processes the PACAP precursor to the mature PACAP-38 and PACAP-27 C-terminally α-amidated forms (Vaudry et al., 2000). Thus we have found coordinate upregulation of a neuropeptide hormone and the enzyme required to convert it to its active form.

PACAP is expressed in many nuclei in the limbic system and the cortex, but its roles outside the hypothalamus have only recently begun to be studied: PACAP has been shown to increase tyrosine hydroxylase (TH) protein activity and mRNA levels in vivo, in primary cell cultures, and in a dissociated rat nucleus accumbens preparation (Moser et al., 1999; Vaudry et al., 2000, and references therein). Intracerebroventricular injection of PACAP increased dopamine release in the hypothalamus in sheep (Anderson and Curlewis, 1998), but it has not been tested whether PACAP can also potentiate dopamine signaling in nigral and ventral tegmental neurons in vivo. The present study found that the gene for GTP cyclohydrolase (*GCH*) is upregulated by inositol depletion. GCH is the rate-limiting enzyme in the synthesis of tetrahydrobiopterin (BH_4), which is the cofactor for TH (Hyland et al., 2003). Synthesis of BH_4 is a limiting factor for TH activity, and mutations in *GCH* cause dopa-responsive dystonia (Hyland et al., 2003). Indeed, chronic treatment with lithium was found to increase TH protein levels in rat brain hippocampus and striatum, and to a minor extent in cortex (Chen et al., 1998).

Two recent small-scale placebo controlled studies demonstrated antidepressant efficacy for pramipexole, a dopamine D2/D3 receptor agonist, as an add-on treatment in bipolar disorder (Goldberg et al., 2004; Zarate et al., 2004). Taken together, the above observations suggest a coordinated upregulation of genes leading to increased dopamine signaling. In the light of the recent clinical data and human genetic linkage studies, it is tempting to speculate that PACAP might be a therapeutic effector of lithium in bipolar disorder.

It is important to point out that we cannot yet say whether the therapeutic action of lithium is mediated by inhibition of IMPase, or GSK3β, or in fact any other molecular target. Indeed, it is possible that inhibition of both IMPase and GSK3β is required. The present study did not, and by its design could not, assess the contribution of GSK3β inhibition to gene regulation, which is expected to be considerable. Very recently, Klein and coworkers have begun to dissect the molecular targets associated with certain lithium-sensitive behaviors using wild-type and GSK3β mutant mice. Their data point to GSK3β as the relevant target of lithium in the forced-swim test, which is a widely recognized predictor of antidepressant/anxiolytic-like drug efficacy (O'Brien et al., 2004).

Conclusion

The most interesting finding in this study is that inositol depletion effected by treatment with an agonist that causes PI turnover and blockade of IMPase by lithium led to upregulation of the *Adcyap1* (PACAP), *Pam*, and *Gch* genes. This trio of genes suggests that modulation of dopamine signaling via regulation of TH activity would be a consequence of inositol depletion in the brain. These findings suggest several lines of experiments. Does chronic lithium treatment in rodents cause changes in brain PACAP levels, and is this brain region- and cell-specific? Is PACAP elevated in brains of IMPase knockout mice? Are PACAP levels in patients with bipolar disorder (measured in the cerebrospinal fluid) different than controls, and is this affected by medication with lithium? Do changes in PACAP correlate with symptomatic relief? In summary, the data presented here warrant further investigation of PACAP signaling in the brain and of the orphan receptor GPR88 as potential new targets in bipolar disorder.

Experimental Procedures

Cortical Slice Culture

All animal procedures were approved by the Institutional Animal Care and Use Committee of Merck Research Laboratories. Male Sprague-Dawley rats (~200 g, 7–8 weeks of age) were euthanized by CO_2 inhalation for 90 s and then decapitated. The brain was rapidly dissected out and placed in ice-cold Krebs-Ringer buffer (KRB: 1.2 mM KH_2PO_4, 118 mM NaCl, 4.7 mM KCl, 1.2 mM $MgSO_4$, 2.5 mM $CaCl_2$, 25 mM $NaHCO_3$, 11 mM D-glucose), which was continuously bubbled with 95% O_2/5% CO_2 (carbogen). The right cerebral cortex was rapidly dissected and chopped into 350 μm coronal slices using a McIlwain tissue chopper (Stoetling Co.). All slices, except the anterior and posterior two to three, were collected into carbogen-bubbled ice-cold KRB and dispensed randomly to culture plates (two per well). This process reliably generated 24 slices per animal, enough for 12 tests. Slices were maintained on porous membrane inserts (Millipore PICM 030 50) at the gas-liquid interface in Neurobasal-A medium (Invitrogen) with 1X B27 supplement (Invitrogen) in polystyrene 6-well plates (Corning Costar). Neurobasal-A/B27 contains 38 μM inositol. The culture plates were held in a tissue culture incubator at 34°C in a custom-made perspex box that was maintained under a slight positive pressure of humified carbogen. One animal was processed per day. These methods were based upon those described previously (Banker and Goslin, 1998; Wilhelmi et al., 2002).

Biochemical Studies, RNA Preparation, and Slice Staining

LiCl, carbachol, D-*myo*-inositol, and 5-[^{3}H]-cytidine (solution in 2% ethanol, 15–25 Ci/mmol, 1 mCi/ml) were purchased from Sigma. CDP-DAG was estimated essentially as described by Atack et al. (1993). Briefly, the membrane inserts holding the radiolabeled slices were transferred to an empty 6-well plate and 1 ml of 1:2 $CHCl_3$/MeOH as added to each well. Slices were transferred with the solvent into 4 ml glass vials (Fisher Scientific) and incubated at

room temperature for 15 min. $CHCl_3$ (0.8 ml) and water (0.8 ml) were added followed by vigorous vortexing for 10 s. Phases were separated by centrifugation, and the organic phase was transferred to a 2 ml plastic tube and washed with 1 ml of 1:1 1 M HCl/MeOH. Finally 0.2 ml of the organic phase was mixed with 5 ml scintillation fluid (Ready-Safe, Beckman) and counted using a Liquid Scintillation Analyzer (Packard).

Total RNA was extracted and purified from slices using the Qiagen RNeasy purification kit. Slices were rinsed with 1 ml cold PBS and transferred to a new tube with 0.6 ml kit lysis buffer. Slices were homogenized using a hand-held homogenizer (PowerGen 125, Fisher) for 3 × 10 s on ice. RNA was purified following the manufacturer's instructions, but with an additional DNase I treatment using the Ambion DNA-*free* kit following the manufacturer's instructions. RNA was finally eluted in 40–50 μl diethylpyrocarbonate-treated (DEPC) water. RNA concentration was measured by UV spectrophotometry, and RNA quality was measured using Agilent's 2100 Bioanalyzer and RNA 6000 Nano LabChip.

Brain slices were stained either immediately after sectioning or after 1 day with various treatments. Slices were rinsed once with KRB/HEPES (KRB as described above, but with 15 mM $NaHCO_3$ and 10 mM HEPES) and incubated at room temperature (RT) either for 5 min in 2.5 ml of 5 μg/ml Hoechst 33342 (Molecular Probes) or for 3 min in 2.5 ml of 4 μM propidium iodide (Molecular Probes) both in KRB/HEPES. Slices were rinsed once with KRB/HEPES at RT (Hoechst staining) or three times (propidium iodide staining) and transferred to 6-well plates with fresh KRB/HEPES for microscopy. Slices were imaged using a Bio-Rad Radiance 2100 confocal laser-scanning system coupled to a Nikon E600FN microscope using a 40× water-immersion objective. Propidium iodide was imaged using one-photon excitation with a 543 nm Green HeNe laser, and emitted light was collected using a 570 nm long-pass filter. Hoechst dye was excited using two-photon excitation at 780 nm from a Coherent Mira-verdi laser source, and emitted light was collected using a 410–490 nm bandpass filter. Infrared light was blocked from reaching the PMT using a 625 nm short-pass filter. Images were acquired at 2 μm intervals. A single maximal-intensity projection image was processed using Image-Pro to count bright objects, corresponding to nuclei. The number and diameter of positively stained nuclei were quantified in 155 × 155 μm regions.

Microarray Profiling

The protocol used for sample amplification and labeling utilizes two rounds of a modified MMLV-RT-mediated reverse transcription protocol (Shannon, 2000). All samples were processed in parallel using a Biomek FX liquid-handling robot. DNase-treated total RNA samples were quantified using RiboGreen (Molecular Probes) as described by the manufacturer. One hundred ng of total RNA and 0.4 pmol of T7T18VN primer (5′ AATTAATACGACTCACTATAGGGAG ATTTTTTTTTTTTTTTTTVN 3′, V = G, C, or T; N = A, G, C, or T) were combined and brought to a final volume of 10.5 μl with water. The RNA was denatured, and the primer was annealed by heating the sample to 65°C for 10 min followed by cooling to 4°C for 5 min. The following components were added to the concentrations listed up to a final reaction volume of 20 μl: 50 mM Tris (pH 8.3), 75 mM KCl, 3 mM $MgCl_2$, 4 U/μl RNAGuard, 0.5 mM each dNTP (dATP, dCTP, dGTP, dTTP), 1.0 ng/μl random hexamers, 10 mM dithiothreitol, and 2.5 U/μl MMLV-RT. The reaction was incubated for 2 hr at 40°C to generate double-stranded cDNA. The MMLV enzyme was denatured by heating the reaction at 65°C for 15 min. For the first in vitro transcription (IVT), the total volume of the reaction was increased to 80 μl with the following components to the final concentrations listed: 40 mM Tris (pH 7.5), 10.0 mM NaCl, 2.0 mM spermidine, 14.25 mM $MgCl_2$, 200 U/ml RNAGuard, 2.5 mM each NTP (ATP, GTP, CTP, UTP), 7.5 mM dithiothreitol, 25 kU/ml T7 RNA polymerase, and 15 U/ml inorganic pyrophosphatase. The IVT reaction was incubated for 4 hr at 40°C. The cRNA from the IVT reaction was purified using the 96-well Qiagen RNeasy purification kit. The cRNA was quantified using UV spectrophotometry and then evaporated using an evaporative centrifuge at 50°C.

The cRNA was rehydrated with 10 μl of 0.27 μg/μl random 9-mers followed by heating to 65°C for 10 min and cooling to 4°C for 5 min. For cDNA synthesis, the reaction volume was increased to 35 μl with the following components to the listed concentrations: 50 mM Tris (pH 8.3), 75 mM KCl, 8 mM $MgCl_2$, 0.5 mM each dNTP (dATP, dCTP, dGTP, dTTP), 10 mM dithiothreitol, and 5.0 U/μl SuperScript II. The generation of the cDNA:cRNA duplex is accomplished by incubating the reaction for 1 hr at 42°C. A size-exclusion filter (Millipore Multiscreen) was used to remove unincorporated random 9-mers. Four pmol of T7T18VN primer were added, and the entire mixture was evaporated using an evaporative centrifuge at 50°C.

The cDNA:cRNA and primer were rehydrated with 10.5 μl of water followed by heating the sample to 65°C for 10 min, followed by cooling to 4°C for 5 min. The following components were added to the concentrations listed in a final reaction volume of 20 μl: 50 mM Tris (pH 8.3), 75 mM KCl, 3 mM $MgCl_2$, 4 U/μl RNAGuard, 0.5 mM each dNTP (dATP, dCTP, dGTP, dTTP), 1.0 ng/μl random hexamers, 10 mM dithiothreitol, and 2.5 U/μl MMLV-RT. This reaction was incubated for 2 hr at 40°C to denature the cRNA and generate double-stranded cDNA. The enzyme was denatured by heating the reaction at 65°C for 15 min. For the IVT, the total volume of the reaction was increased to 80 μl with the following components at the concentrations listed: 40 mM Tris (pH 7.5), 10.0 mM NaCl, 2.0 mM spermidine, 14.25 mM $MgCl_2$, 200 U/ml RNAGuard, 2.5 mM each (ATP, CTP, GTP), 1.88 mM UTP, 0.6 mM amino-allyl UTP, 7.5 mM dithiothreitol, 25 kU/ml T7 RNA polymerase, and 15 U/ml inorganic pyrophosphatase. The label-incorporating IVT reaction was incubated for 16 hr at 40°C. The cRNA from the in vitro transcription reaction was purified using a 96-well Qiagen RNeasy purification kit and quantified using UV spectrophotometer.

The final amino-allyl-cRNA was coupled to CyDye molecules, fragmented, and hybridized to custom 60-mer oligonucleotide microarrays (Agilent) as described (Hughes et al., 2001). Each sample was separately coupled to Cy3 and Cy5 and hybridized to the oppositely coupled control sample. Thus, each pair of samples was analyzed on two separate microarrays, termed a fluor-reversed pair (FRP). The arrays were scanned using an Agilent DNA Microarray Scanner, and array images were analyzed using custom Matlab programs.

Microarray Data Analysis

The general quality of the hybridizations was excellent. However, five samples were hybridized to new arrays when their initial hybridizations did not meet our stringent standards. Since the expression data from the new hybridizations were highly correlated with data from the initial hybridizations, to gain precision we calculated weighted averages between the two, with weights based on the reciprocal of the estimated measurement variance, and used the weighted averages for all downstream analysis. Any reporter that failed to give reliable data for five or more samples was deemed unreliable and not analyzed.

An analysis of variance (ANOVA) model was fit separately to the log ratios (Treatment versus LiCl + carbachol reference pool) for each of the remaining 23,251 reporters. The ANOVA model contained terms for both treatment (LiCl, LiCl + carbachol, or LiCl + carbachol + inositol) and animal (1 or 2). Estimates of differences (or fold changes) were obtained from the means calculated in the ANOVA fit. Tests of significance were performed using a t statistic constructed from these difference estimates and an empirical bayesian estimate of error (Smyth, 2004). The strength of this approach is that for a particular gene, the error estimate is a combination of a gene-specific error estimate and a global error estimate across all the genes.

RT-QPCR

Messenger RNA was amplified to produce antisense RNA (aRNA) based on protocols developed by Eberwine and coworkers (Phillips and Eberwine, 1996). All 36 samples were processed in parallel. Total RNA (0.8 μg) was used to prepare double-stranded (ds)-cDNA using the SuperScript Double-Stranded cDNA Synthesis kit (Invitrogen) with oligo-dT primers containing a T7 polymerase promoter sequence (5′-GGCCAGTGAATTGTAATACGACTCACTATAGGGAGG $CGGT_{24}$-3′) following the manufacturer's instructions except that the final concentration of primer was 1 μM and we added 0.25 μl of 40 units/μl RNASEOUT Ribonuclease Inhibitor (Invitrogen 10777-

019) in the first strand synthesis step without changing the reaction volume. Product ds-cDNA was purified using the MiniElute Reaction Cleanup kit (Qiagen) following the manufacturer's instructions. The AmpliScribe T7 Transcription (Epicentre) kit was used to prepare aRNA by in vitro transcription from the total ds-cDNA from each sample according to the manufacturer's instructions with the following exceptions: we scaled up the reaction mixture 2-fold, we used 4 μl of 1000 units/μl T7 RNA polymerase (Epicentre TH950k) per reaction, and we included 0.5 μl of 40 units/μl RNASEOUT Ribonuclease Inhibitor in each reaction. The reaction was incubated at 37°C for 4 hr. RNA was purified using the RNeasy Mini kit (Qiagen). RNA concentration was measured by UV spectrophotometry, and RNA quality was measured using Agilent's 2100 Bioanalyzer and RNA 6000 Nano LabChip.

One μg of aRNA per sample was used to prepare the cDNA PCR template using 1 μg random hexamer primer (Invitrogen 48190-011), using the first-strand synthesis portion of the SuperScript Double-Stranded cDNA Synthesis kit (Invitrogen) following the manufacturer's instructions.

PCR reactions were carried out in 384-well plates using the Assays-on-Demand Gene Expression Products protocols available from Applied Biosystems using the cDNA derived from 2 ng aRNA per reaction. Custom-designed primers and probes were used at 200 nM. Reaction components were added to assay plates using a Beckman-Coulter MultiMek pipeting robot. The commercial assays and custom-prepared primer/probe sets used in this study are summarized in Table S2.

Each aRNA sample was tested for contamination with DNA by running a small sample through the cDNA synthesis reaction without reverse transcriptase, and running RT-QPCR assays for *β-2 microglobulin* (*B2m*), *glucuronidase β* (*Gusb*), and *Jun*. None of the samples were contaminated.

We used multiple endogenous reference genes in the RT-QPCR experiment to build redundancy into this aspect of the analysis. This required the analysis to be carried out in a one plate–one RNA–many genes configuration, which in turn necessitates comparison of ΔC_t values across plates. We validated this experimentally (data not shown). Two rat genes recommended as endogenous references by Applied Biosystems Inc. are *B2m* and *Gusb*. Neither of these genes were regulated by the treatments based on the microarray data set (data not shown). Two other genes, *vesicle-associated membrane protein 1* (*Vamp1*) and *X-ray repair cross-complementing group 1 protein* (*Xrcc1*), were identified in the microarray data set as being very confidently not differentially expressed across treatments (data not shown).

Samples (one per plate) were analyzed sequentially as blocks of samples grouped by animal. Each block took 3 days (maximum three plates per day) to process, and a fresh batch of reagents was prepared for each block. Within each block, the sample order was randomized using a Latin square design, with a different design for each block. In this way, between animal, between day of sacrifice, and between reagent batch variabilities were segregated together, whereas interplate variability was randomized across samples and treatments. Four technical replicates were performed for each assay.

In addition to test wells, every plate included an assay of *B2m* in a cDNA sample derived from RNA from rat cortical slice tissue processed in the same way as the test samples. These wells were used to set a consistent plate-to-plate threshold fluorescence level for the determination of C_t, even though C_t is theoretically independent of the threshold setting.

RT-QPCR Data Analysis

Three of the 33 samples analyzed by RT-QPCR were not used due to quality control indications. The data for different genes were not pooled; each gene was analyzed independently of all others. The two sets of data for the *Crem* gene were also analyzed separately. ΔC_t values were calculated using a means-normalized aggregate of three endogenous reference genes (*B2m*, *Gusb*, and *Xrcc1*). For each set of gene data, a mixed linear model (Searle et al., 1992) was fit with $\Delta\Delta C_t$ as the dependent variable, the three treatments as fixed effects, and both animal and plate as separate random effects. Two-sided p values were obtained for the treatment differences LC versus L and LCI versus LC, based on the error structure of the mixed model. R software (version 1.9.1, http://www.r-project.org/) and the nlme package (version 7.1-48; Pinhiero and Bates, 2000) were used to perform the analyses. The results of the analysis are reported in Table S3, including the derived value for the mean $\Delta\Delta C_t$ and the standard error of that mean value. The fold change is equal to 2 raised to the power of the numerical value of $\Delta\Delta C_t$.

Supplemental Data

The Supplemental Data and Conflict of Interest Statement that accompany this article can be found online at http://www.neuron.org/cgi/content/full/45/6/861/DC1/.

Acknowledgments

We acknowledge Andrea Yost and Jon R. Oblad for excellent technical support, as well as other Rosetta Gene Expression Lab personnel. We acknowledge use of the Online Mendelian Inheritance in Man (OMIM) annotated database in mining of the inositol-regulated gene list (http://www.ncbi.nlm.nih.gov/entrez/query.fcgi?db=OMIM). The authors have declared a conflict of interest. For details, see http://www.neuron.org/cgi/content/full/45/6/861/DC1/.

Received: September 21, 2004
Revised: December 21, 2004
Accepted: February 2, 2005
Published: March 23, 2005

References

Allison, J.H., and Stewart, M.A. (1971). Reduced brain inositol in lithium-treated rats. Nat. New Biol. *233*, 267–268.

Anderson, S.T., and Curlewis, J.D. (1998). PACAP stimulates dopamine neuronal activity in the medial basal hypothalamus and inhibits prolactin. Brain Res. *790*, 343–346.

Atack, J.R., Cook, S.M., Watt, A.P., and Ragan, C.I. (1992). Measurement of lithium-induced changes in mouse inositol(1)phosphate levels in vivo. J. Neurochem. *59*, 1946–1954.

Atack, J.R., Prior, A.M., Griffith, D., and Ragan, C.I. (1993). Characterization of the effects of lithium on phosphatidylinositol (PI) cycle activity in human muscarinic m1 receptor-transfected CHO cells. Br. J. Pharmacol. *110*, 809–815.

Banker, G., and Goslin, K. (1998). Culturing Nerve Cells (Cambridge, MA: The MIT Press).

Berridge, M.J., Downes, C.P., and Hanley, M.R. (1989). Neural and developmental actions of lithium: a unifying hypothesis. Cell *59*, 411–419.

Bonde, C., Noraberg, J., and Zimmer, J. (2002). Nuclear shrinkage and other markers of neuronal cell death after oxygen-glucose deprivation in rat hippocampal slice cultures. Neurosci. Lett. *327*, 49–52.

Bowden, C.L., Calabrese, J.R., McElroy, S.L., Gyulai, L., Wassef, A., Petty, F., Pope, H.G., Jr., Chou, J.C., Keck, P.E., Jr., Rhodes, L.J., et al. (2000). A randomized, placebo-controlled 12-month trial of divalproex and lithium in treatment of outpatients with bipolar I disorder. Divalproex Maintenance Study Group. Arch. Gen. Psychiatry *57*, 481–489.

Bowden, C.L., Calabrese, J.R., Sachs, G., Yatham, L.N., Asghar, S.A., Hompland, M., Montgomery, P., Earl, N., Smoot, T.M., and DeVeaugh-Geiss, J. (2003). A placebo-controlled 18-month trial of lamotrigine and lithium maintenance treatment in recently manic or hypomanic patients with bipolar I disorder. Arch. Gen. Psychiatry *60*, 392–400.

Burgess, S., Geddes, J., Hawton, K., Townsend, E., Jamison, K., and Goodwin, G. (2003). Lithium for maintenance treatment of mood disorders (Cochrane Review). In The Cochrane Library, Issue 4 (Chichester, UK: John Wiley & Sons, Ltd).

Chen, G., Yuan, P.X., Jiang, Y.M., Huang, L.D., and Manji, H.K.

(1998). Lithium increases tyrosine hydroxylase levels both in vivo and in vitro. J. Neurochem. *70*, 1768–1771.

Detera-Wadleigh, S.D., Badner, J.A., Berrettini, W.H., Yoshikawa, T., Goldin, L.R., Turner, G., Rollins, D.Y., Moses, T., Sanders, A.R., Karkera, J.D., et al. (1999). A high-density genome scan detects evidence for a bipolar-disorder susceptibility locus on 13q32 and other potential loci on 1q32 and 18p11.2. Proc. Natl. Acad. Sci. USA *96*, 5604–5609.

Dinan, T.G. (2002). Lithium in bipolar mood disorder. BMJ *324*, 989–990.

DSM-IV(1994). Diagnostic and Statistical Manual of Mental Disorders (DSM-IV) (Wasington, DC: American Psychiatric Association).

Godfrey, P.P. (1989). Potentiation by lithium of CMP-phosphatidate formation in carbachol-stimulated rat cerebral-cortical slices and its reversal by myo-inositol. Biochem. J. *258*, 621–624.

Goldberg, J.F., Burdick, K.E., and Endick, C.J. (2004). Preliminary randomized, double-blind, placebo-controlled trial of pramipexole added to mood stabilizers for treatment-resistant bipolar depression. Am. J. Psychiatry *161*, 564–566.

Goodwin, F.K., Fireman, B., Simon, G.E., Hunkeler, E.M., Lee, J., and Revicki, D. (2003). Suicide risk in bipolar disorder during treatment with lithium and divalproex. JAMA *290*, 1467–1473.

Gould, T.D., Quiroz, J.A., Singh, J., Zarate, C.A., and Manji, H.K. (2004). Emerging experimental therapeutics for bipolar disorder: insights from the molecular and cellular actions of current mood stabilizers. Mol. Psychiatry *9*, 734–755.

Gray, S.L., Yamaguchi, N., Vencova, P., and Sherwood, N.M. (2002). Temperature-sensitive phenotype in mice lacking pituitary adenylate cyclase-activating polypeptide. Endocrinology *143*, 3946–3954.

Gurvich, N., and Klein, P.S. (2002). Lithium and valproic acid: parallels and contrasts in diverse signaling contexts. Pharmacol. Ther. *96*, 45–66.

Hashimoto, H., Shintani, N., Tanaka, K., Mori, W., Hirose, M., Matsuda, T., Sakaue, M., Miyazaki, J., Niwa, H., Tashiro, F., et al. (2001). Altered psychomotor behaviors in mice lacking pituitary adenylate cyclase-activating polypeptide (PACAP). Proc. Natl. Acad. Sci. USA *98*, 13355–13360.

Hashimoto, H., Shintani, N., and Baba, A. (2002). Higher brain functions of PACAP and a homologous Drosophila memory gene amnesiac: insights from knockouts and mutants. Biochem. Biophys. Res. Commun. *297*, 427–431.

Hughes, T.R., Mao, M., Jones, A.R., Burchard, J., Marton, M.J., Shannon, K.W., Lefkowitz, S.M., Ziman, M., Schelter, J.M., Meyer, M.R., et al. (2001). Expression profiling using microarrays fabricated by an ink-jet oligonucleotide synthesizer. Nat. Biotechnol. *19*, 342–347.

Hyland, K., Gunasekara, R.S., Munk-Martin, T.L., Arnold, L.A., and Engle, T. (2003). The hph-1 mouse: a model for dominantly inherited GTP-cyclohydrolase deficiency. Ann. Neurol. *54*, 46–48.

Irvine, R.F., and Schell, M.J. (2001). Back in the water: the return of the inositol phosphates. Nat. Rev. Mol. Cell Biol. *2*, 327–338.

Jope, R.S., and Bijur, G.N. (2002). Mood stabilizers, glycogen synthase kinase-3beta and cell survival. Mol. Psychiatry *7*, 35–45.

Kawaguchi, C., Tanaka, K., Isojima, Y., Shintani, N., Hashimoto, H., Baba, A., and Nagai, K. (2003). Changes in light-induced phase shift of circadian rhythm in mice lacking PACAP. Biochem. Biophys. Res. Commun. *310*, 169–175.

Kristensen, B.W., Noer, H., Gramsbergen, J.B., Zimmer, J., and Noraberg, J. (2003). Colchicine induces apoptosis in organotypic hippocampal slice cultures. Brain Res. *964*, 264–278.

Lenox, R.H., and Manji, H.K. (1998). Lithium. In Textbook of Psychopharmacology, A. Schatzberg and C. Nemeroff, eds. (Washington, DC: The American Psychiatric Press).

Lenox, R.H., Gould, T.D., and Manji, H.K. (2002). Endophenotypes in bipolar disorder. Am. J. Med. Genet. *114*, 391–406.

Loewen, C.J., Gaspar, M.L., Jesch, S.A., Delon, C., Ktistakis, N.T., Henry, S.A., and Levine, T.P. (2004). Phospholipid metabolism regulated by a transcription factor sensing phosphatidic acid. Science *304*, 1644–1647.

Lubrich, B., Patishi, Y., Kofman, O., Agam, G., Berger, M., Belmaker, R.H., and van Calker, D. (1997). Lithium-induced inositol depletion in rat brain after chronic treatment is restricted to the hypothalamus. Mol. Psychiatry *2*, 407–412.

Majerus, P.W. (1992). Inositol phosphate biochemistry. Annu. Rev. Biochem. *61*, 225–250.

McInnes, L.A., Service, S.K., Reus, V.I., Barnes, G., Charlat, O., Jawahar, S., Lewitzky, S., Yang, Q., Duong, Q., Spesny, M., et al. (2001). Fine-scale mapping of a locus for severe bipolar mood disorder on chromosome 18p11.3 in the Costa Rican population. Proc. Natl. Acad. Sci. USA *98*, 11485–11490.

Mikkelsen, J.D., Hannibal, J., Larsen, P.J., and Fahrenkrug, J. (1994). Pituitary adenylate cyclase activating peptide (PACAP) mRNA in the rat neocortex. Neurosci. Lett. *171*, 121–124.

Mizushima, K., Miyamoto, Y., Tsukahara, F., Hirai, M., Sakaki, Y., and Ito, T. (2000). A novel G-protein-coupled receptor gene expressed in striatum. Genomics *69*, 314–321.

Moser, A., Scholz, J., and Gansle, A. (1999). Pituitary adenylate cyclase-activating polypeptide (PACAP-27) enhances tyrosine hydroxylase activity in the nucleus accumbens of the rat. Neuropeptides *33*, 492–497.

Nonaka, S., Hough, C.J., and Chuang, D.M. (1998). Chronic lithium treatment robustly protects neurons in the central nervous system against excitotoxicity by inhibiting N-methyl-D-aspartate receptor-mediated calcium influx. Proc. Natl. Acad. Sci. USA *95*, 2642–2647.

O'Brien, W.T., Harper, A.D., Jove, F., Woodgett, J.R., Maretto, S., Piccolo, S., and Klein, P.S. (2004). Glycogen synthase kinase-3beta haploinsufficiency mimics the behavioral and molecular effects of lithium. J. Neurosci. *24*, 6791–6798.

Ogden, C.A., Rich, M.E., Schork, N.J., Paulus, M.P., Geyer, M.A., Lohr, J.B., Kuczenski, R., and Niculescu, A.B. (2004). Candidate genes, pathways and mechanisms for bipolar (manic-depressive) and related disorders: an expanded convergent functional genomics approach. Mol. Psychiatry *9*, 1007–1029.

Phillips, J., and Eberwine, J.H. (1996). Antisense RNA Amplification: A Linear Amplification Method for Analyzing the mRNA Population from Single Living Cells. Methods *10*, 283–288.

Pinhiero, J., and Bates, D. (2000). Mixed-Effects Models in S and S-Plus (New York: Springer).

Ren, M., Senatorov, V.V., Chen, R.W., and Chuang, D.M. (2003). Postinsult treatment with lithium reduces brain damage and facilitates neurological recovery in a rat ischemia/reperfusion model. Proc. Natl. Acad. Sci. USA *100*, 6210–6215.

Schuller, H.J., Richter, K., Hoffmann, B., Ebbert, R., and Schweizer, E. (1995). DNA binding site of the yeast heteromeric Ino2p/Ino4p basic helix-loop-helix transcription factor: structural requirements as defined by saturation mutagenesis. FEBS Lett. *370*, 149–152.

Searle, S.R., Casella, G., and McCulloch, C. (1992). Variance Components (Hoboken, NJ: Wiley).

Shannon, K.W. (2000). Method for Linear mRNA Amplification. [US 6,132,997].

Sherman, W.R., Gish, B.G., Honchar, M.P., and Munsell, L.Y. (1986). Effects of lithium on phosphoinositide metabolism in vivo. Fed. Proc. *45*, 2639–2646.

Skoglosa, Y., Takei, N., and Lindholm, D. (1999). Distribution of pituitary adenylate cyclase activating polypeptide mRNA in the developing rat brain. Brain Res. Mol. Brain Res. *65*, 1–13.

Smyth, G.K. (2004). Linear models and empirical Bayes methods for assessing differential expression in microarray experiments. Statistical Applications in Genetics and Molecular Biology *3*, Article 3. http://www.bepress.com/sagmb/vol3/iss1/art3.

Stubbs, E.B., Jr., and Agranoff, B.W. (1993). Lithium enhances muscarinic receptor-stimulated CDP-diacylglycerol formation in inositol-depleted SK-N-SH neuroblastoma cells. J. Neurochem. *60*, 1292–1299.

Vaden, D.L., Ding, D., Peterson, B., and Greenberg, M.L. (2001). Lithium and valproate decrease inositol mass and increase expression of the yeast INO1 and INO2 genes for inositol biosynthesis. J. Biol. Chem. *276*, 15466–15471.

Vaudry, D., Gonzalez, B.J., Basille, M., Yon, L., Fournier, A., and Vaudry, H. (2000). Pituitary adenylate cyclase-activating polypeptide and its receptors: from structure to functions. Pharmacol. Rev. *52*, 269–324.

Wang, L., Liu, X., and Lenox, R.H. (2001). Transcriptional downregulation of MARCKS gene expression in immortalized hippocampal cells by lithium. J. Neurochem. *79*, 816–825.

Weissman, M.M., Leaf, P.J., Tischler, G.L., Blazer, D.G., Karno, M., Bruce, M.L., and Florio, L.P. (1988). Affective disorders in five United States communities. Psychol. Med. *18*, 141–153.

Welsh, D.K., and Moore-Ede, M.C. (1990). Lithium lengthens circadian period in a diurnal primate, Saimiri sciureus. Biol. Psychiatry *28*, 117–126.

Wilhelmi, E., Schoder, U.H., Benabdallah, A., Sieg, F., Breder, J., and Reymann, K.G. (2002). Organotypic brain-slice cultures from adult rats: approaches for a prolonged culture time. Altern. Lab. Anim. *30*, 275–283.

Zarate, C.A., Jr., Payne, J.L., Singh, J., Quiroz, J.A., Luckenbaugh, D.A., Denicoff, K.D., Charney, D.S., and Manji, H.K. (2004). Pramipexole for bipolar II depression: a placebo-controlled proof of concept study. Biol. Psychiatry *56*, 54–60.